Single-carrier Media-based Modulation in ISI Channels

Swaroop Jacob and A. Chockalingam
Department of ECE, Indian Institute of Science, Bangalore 560012

***Abstract*—A promising modulation scheme called *media-based modulation (MBM)* is attracting recent research attention. In MBM, radio frequency (RF) mirrors (parasitic elements) are placed near the transmit antenna in order to create different channel fade realizations based on the ON/OFF status of these mirrors, and the resulting complex fade realizations constitute the MBM channel alphabet. The key advantages of MBM are: i) the number of bits conveyed through the choice of the OF/OFF status of the mirrors *increases linearly* with the number of RF mirrors, and ii) it possesses very good performance attributes due to the additive properties of information over multiple receive antennas. In this paper, we present a study of MBM in ISI channels with a focus on cyclic prefixed single carrier (CPSC) systems. Our new contributions in this paper can be summarized as follows: i) it is shown that, for the same spectral efficiency, CPSC-MBM scheme can outperform conventional OFDM and CPSC schemes, ii) an eigen-value based diversity analysis of the CPSC-MBM scheme is presented; simulation results validate the analytically obtained diversity orders, and iii) a novel message passing based low-complexity algorithm for CPSC-MBM signal detection that scales well and achieves good performance is proposed.**

Keywords *– Media-based modulation, index modulation, RF mirrors, frequency-selective fading, single-carrier systems.*

I. Introduction

The use of parasitic elements external to antennas in radio frequency (RF) wireless communications is known to have several applications [1]-[4]. The parasitic elements include capacitors, varactors or switched capacitors that can adjust the resonance frequency. A widely known application is the use of parasitic elements for beamforming purposes [1]. Other applications include direction of arrival (DoA) estimation [2], achieving selection/switched diversity [3], and reconfigurable antennas [4]. Another interesting application that is of interest for our work in this paper is the idea of conveying information bits through antenna pattern indexing [5],[6]. The *aerial modulation* scheme studied in [5] uses indexing orthogonal antenna patterns realized using a single antenna surrounded by parasitic elements to convey information bit(s) in addition to bits conveyed through an M-PSK symbol. On similar lines, recently, the *media-based modulation (MBM)* proposed in [7] exploits the idea of indexing a multiplicity of complex channel fades realized by placing RF mirrors (parasitic elements) near the transmit antenna and allowing information bits to control the transparent/opaque status of these mirrors. The different complex channel fades corresponding to different combinations of mirror control bits form the MBM channel alphabet.

In MBM, the RF mirrors can be made ON or OFF based on information bits. An ON status of a RF mirror implies that the mirror allows the incident wave to pass through it, and an OFF status implies that the incident wave is reflected back. Assuming a rich scattering environment, a small perturbation in the environment caused by the ON/OFF status of these mirrors will be augmented by multiple reflections resulting in different channel fades. Let us call a given realization of the ON/OFF status of the RF mirrors as the 'mirror activation pattern' (MAP). Each of the MAPs creates a different channel fade realization. In addition to the bits conveyed through conventional modulation symbols (e.g., QAM/PSK symbols), selection of the MAP conveys additional information bits in MBM. This allows MBM to achieve increased rates.

Consider a single antenna system. Assume that there are m_{rf} RF mirrors placed near the transmit antenna. There are $2^{m_{rf}}$ possible MAPs, and a MAP to be used in a given channel use can be selected using m_{rf} bits. Therefore, MBM can convey m_{rf} information bits in one channel use through RF mirror indexing. This means that the achieved rate in bits per channel use (bpcu) in MBM *scales linearly with the number of RF mirrors used*. This is a key advantage of MBM. The MBM channel alphabet (i.e., $2^{m_{rf}}$ fade realizations corresponding to all the MAPs) needs to be known at the receiver for signal detection. This can be estimated through pilot transmission. The number of pilot channel uses needed increases exponentially with m_{rf}. This is a key issue in MBM.

In addition to the rate advantage due to mirror indexing, MBM can achieve performance advantage as well. For the same bpcu, MBM has been shown to achieve better performance compared to conventional modulation schemes [7]-[10]. It has been shown that MBM with one transmit and n_r receive antennas over a multipath channel asymptotically (as $m_{rf} \rightarrow \infty$) achieves the capacity of n_r parallel AWGN channels [8]. The performance of MBM with multiple transmit antennas (MIMO-MBM) has been studied in [10], where it has been shown that MIMO-MBM can achieve better performance compared to conventional MIMO. This paper also reports an implementation of an MBM transmit unit consisting of 14 RF mirrors placed in a compact cylindrical structure with a dipole transmit antenna element placed at the center of the cylindrical structure. The performance of MBM with generalized spatial modulation (GSM-MBM) is studied in [11], where it is shown that, for the same bpcu, GSM-MBM can perform better than MIMO-MBM.

In this paper, we present a study of MBM in ISI channels. MBM in ISI channels has not been reported before. We consider single-carrier (SC) approach [14],[15], where bits are organized into data frames and each data frame is transmitted

This work was supported in part by the J. C. Bose National Fellowship, Department of Science and Technology, Government of India.

This is in contrast with antenna index modulation schemes like space shift keying (SSK) or spatial modulation (SM), where the bpcu scales only logarithmically with the number of transmit antennas.

along with cyclic prefix (CP) bits which avoids inter-frame interference in ISI channels [16]-[18]. The CP converts linear convolution of the channel with data to circular convolution which is multiplication in frequency domain and this enables low complexity frequency domain processing at the receiver. In this paper, we study cyclic-prefixed single-carrier MBM (CPSC-MBM) systems. Our new contributions in this paper can be summarized as follows:

- First, we show that, for the same spectral efficiency, CPSC-MBM scheme can outperform conventional OFDM and CPSC schemes.
- Next, we present an eigen-value based diversity analysis of CPSC-MBM and present simulation results that validate the analytically obtained diversity orders.
- Finally, we present a novel message passing based low-complexity algorithm for CPSC-MBM signal detection that scales well and achieves good performance.

The rest of this paper is organized as follows. The CPSC-MBM system model and maximum likelihood (ML) detection performance for small system sizes are presented in Sec. II. The diversity analysis of the CPSC-MBM system under ML detection is presented in Sec. III. The proposed message passing detection algorithm suited for large system sizes and its performance are presented in Sec. IV. Conclusions are presented in Sec. V.

II. CPSC-MBM SYSTEM MODEL

An MBM transmit unit (MBM-TU) consists of a transmit antenna and m_{rf} RF mirrors placed near it. We consider an MBM system with one MBM-TU at the transmit side and n_r receive antennas at the receive side. The MBM transmitter is shown in Fig. 1. The channel is assumed to be frequency selective with L multipaths with an exponential power delay profile (PDP). Transmission is carried out in frames. Each frame consists of $N+L-1$ channel uses, where N denotes the length of the data part in number of channel uses and $L-1$ channel uses are used for transmitting the CP. In each of the N channel uses, $m_{rf}+\log_2|\mathbb{A}|$ information bits are conveyed, where m_{rf} bits are conveyed through RF mirror indexing and $\log_2|\mathbb{A}|$ bits are conveyed through a symbol from an M-ary modulation alphabet $\mathbb{A}$. That is, in each of the N channel uses, the antenna transmits a symbol from $\mathbb{A}$ (determined by $\log_2|\mathbb{A}|$ information bits) and the ON/OFF status of the RF mirrors, referred to as 'mirror activation pattern' (MAP), is determined by an additional m_{rf} information bits. Therefore, the achieved rate in bits per channel use (bpcu) is given by

$$R = \frac{N}{N+L-1}\Big[\underbrace{m_{rf}}_{\text{mirror index bits}} + \underbrace{\log_2|\mathbb{A}|}_{\text{modulation symbol bits}}\Big] \text{ bpcu.}$$

A. MBM channel alphabet

The MBM channel alphabet is the set of all channel gain vectors corresponding to the various MAPs. Define $N_m \triangleq 2^{m_{rf}}$. The number of possible MAPs is N_m. Let $h_{j,k}^{(l)}$ denote the channel gain from the MBM-TU to the jth receive antenna for the kth MAP on the lth multipath, where

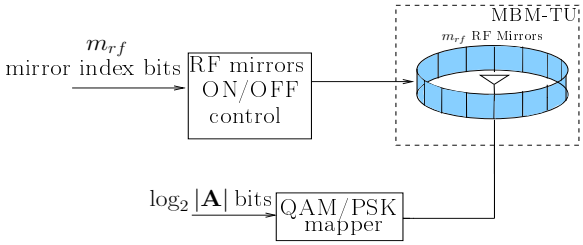

Fig. 1. MBM transmitter.

$h_{j,k}^{(l)} \sim \mathcal{CN}(0,1)$, $j = 1,2,\cdots,n_r$, $l = 0,1,\cdots,L-1$, and $k = 1,2,\cdots,N_m$. The power delay profile of the channel is assumed to follow exponential decaying model, i.e., $\mathbb{E}[|h_{j,k}^{(l)}|^2] = e^{-l}$, $l = 0,1,\cdots,L-1$. Let $\mathbf{h}_k^{(l)} = [h_{1,k}^{(l)}\ h_{2,k}^{(l)}\ \cdots\ h_{n_r,k}^{(l)}]^T$ denote the $n_r \times 1$-sized channel gain vector on the lth multipath for the kth MAP. Define an $n_rL\times 1$-sized vector $\mathbf{h}_k$ as $\mathbf{h}_k = [\mathbf{h}_k^{(0)^T}\mathbf{h}_k^{(1)^T}\cdots\mathbf{h}_k^{(L-1)^T}]^T$. Then the set of the N_m vectors $\{\mathbf{h}_k, k = 1,\cdots,N_m\}$ form the MBM channel alphabet $\mathbb{H}$. The knowledge of the alphabet $\mathbb{H}$ is needed at the receiver for detection, which is obtained through pilot transmission and estimation of $\mathbb{H}$ at the receiver before data transmission.

B. MBM signal set

Define $\mathbb{A}_0 \triangleq \mathbb{A}\cup 0$. The conventional MBM signal set, denoted by $\mathbb{S}$, is the set of $N_m \times 1$-sized MBM signal vectors, which is given by

$$\mathbb{S} = \Big\{\mathbf{s}_{k,q} \in \mathbb{A}_0^{N_m} : k = 1,\cdots,N_m,\ q = 1,\cdots,|\mathbb{A}|\Big\}$$
$$\text{s.t } \mathbf{s}_{k,q} = [0,\cdots,0,\ \underbrace{s_q}_{k\text{th coordinate}}\ 0,\cdots,0]^T, s_q \in \mathbb{A}, \quad (1)$$

where k is the index of the MAP. The size of the MBM signal set is $|\mathbb{S}| = N_m|\mathbb{A}|$. For example, if $m_{rf} = 2$ and $|\mathbb{A}| = 2$ (i.e., BPSK), then the MBM signal set is given by

$$\mathbb{S} = \left\{\begin{bmatrix}1\\0\\0\\0\end{bmatrix}, \begin{bmatrix}-1\\0\\0\\0\end{bmatrix}, \begin{bmatrix}0\\1\\0\\0\end{bmatrix}, \begin{bmatrix}0\\-1\\0\\0\end{bmatrix}, \begin{bmatrix}0\\0\\1\\0\end{bmatrix}, \begin{bmatrix}0\\0\\-1\\0\end{bmatrix}, \begin{bmatrix}0\\0\\0\\1\end{bmatrix}, \begin{bmatrix}0\\0\\0\\-1\end{bmatrix}\right\}. \quad (2)$$

C. CPSC-MBM received signal

In each of the N channel uses, an MBM signal vector from $\mathbb{S}$ is transmitted. Let $\mathbf{x}_i \in \mathbb{S}$ denote the transmitted vector of size $N_m \times 1$ in the ith channel use, $1 \le i \le N+L-1$. We assume that the channel remain invariant in one frame duration. At the receiver, after removing the CP, the received vector can be represented as

$$\mathbf{y} = \mathbf{H}\mathbf{x} + \mathbf{n}, \quad (3)$$

where $\mathbf{n}$ is the noise vector of size $Nn_r \times 1$ with $\mathbf{n} \sim \mathcal{CN}(0,\sigma^2\mathbf{I}_{Nn_r})$, $\mathbf{x}$ is the vector of size $NN_m\times 1$ given by $\mathbf{x} = \begin{bmatrix}\mathbf{x}_L^T & \mathbf{x}_{L+1}^T & \cdots & \mathbf{x}_{N+L-1}^T\end{bmatrix}^T$, and $\mathbf{H}$ is the $Nn_r \times NN_m$

equivalent block circulant channel matrix given by

$$\mathbf{H}=\begin{bmatrix} \mathbf{H}_0 & 0 & 0 & 0 & \cdots & 0 & \mathbf{H}_{L-1} & \cdots & \mathbf{H}_1 \\ \mathbf{H}_1 & \mathbf{H}_0 & 0 & 0 & \cdots & 0 & 0 & \cdots & \mathbf{H}_2 \\ \vdots & \vdots & \vdots & \vdots & \vdots & \vdots & \vdots & \vdots & \\ \mathbf{H}_{L-2} & \mathbf{H}_{L-3} & \mathbf{H}_{L-4} & \cdot & \mathbf{H}_0 & 0 & \cdot & \cdots & \mathbf{H}_{L-1} \\ \mathbf{H}_{L-1} & \mathbf{H}_{L-2} & \mathbf{H}_{L-3} & \cdot & \mathbf{H}_1 & \mathbf{H}_0 & 0 & \cdots & 0 \\ 0 & \mathbf{H}_{L-1} & \mathbf{H}_{L-2} & \cdot & \mathbf{H}_2 & \mathbf{H}_1 & \mathbf{H}_0 & \cdots & 0 \\ \vdots & \vdots & \vdots & \vdots & \vdots & \vdots & \vdots & \vdots & \\ 0 & 0 & 0 & \cdot & \cdot & \cdot & \cdot & \cdots & \mathbf{H}_0, \end{bmatrix},$$

where $\mathbf{H}_l$ is the $n_r \times N_m$ channel matrix corresponding to the lth multipath, whose entry in the jth row and kth column is $h_{j,k}^{(l)}$. The received signal-to-noise ratio (SNR) is given by E_s/σ^2, where E_s is the average symbol energy and σ^2 is the variance of the additive noise.

D. ML detection performance

The ML detection rule is given by

$$\hat{\mathbf{x}} = \underset{\mathbf{x}\in\mathbb{S}_{\text{cpsc-mbm}}}{\text{argmin}} \quad ||\mathbf{y}-\mathbf{H}\mathbf{x}||^2, \tag{4}$$

where $\mathbb{S}_{\text{cpsc-mbm}}$ is the set of all possible $\mathbf{x}$ vectors. The $\hat{\mathbf{x}}$ obtained is demapped to get the MAP on each channel use, which are then demapped to obtain the mirror index bits on each of the N channel uses. The non-zero entries of $\hat{\mathbf{x}}$ are demapped to get the modulation bits transmitted on the N channel uses. Note that the complexity of the ML detection in (4) is exponential in m_{rf} and N.

Figure 2 shows the ML performance of CPSC-MBM with $m_{rf} = 2$, $N = 4$, $n_r = 4$, BPSK, and an achieved rate of 2.4 bpcu. A frequency selective channel with $L = 2$ channel taps with exponential power delay profile given in II-C is considered. We compare this performance with that of conventional OFDM and CPSC schemes. The parameters taken for OFDM and CPSC schemes are $N = 4$, $n_r = 4$, $L = 2$, 8-QAM, and 2.4 bpcu. Note that all the three schemes considered for comparison (i.e., CPSC-MBM, OFDM, and CPSC) use one radio frequency (RF) chain for transmission. From Fig. 2, we observe that, for the same achieved rate of 2.4 bpcu, CPSC-MBM outperforms conventional OFDM and CPSC schemes. At a BER of 10^{-4}, CPSC-MBM outperforms OFDM by about 6.2 dB, and CPSC by about 4.2 dB. This performance advantage is due to the modulation alphabet size difference (BPSK in CPSC-MBM and 8-QAM in OFDM and CPSC) due to the additional mirror index bits in CPSC-MBM, and this results in an SNR advantage in favor of CPSC-MBM. This observed advantage of CPSC-MBM over conventional schemes motivates further investigations on CPSC-MBM. Accordingly, we, in the next two sections, analyze the diversity of CPSC-MBM and develop low complexity detection schemes that scale well for large system sizes.

III. Diversity analysis

In this section, we analyze the diversity order achieved by CPSC-MBM. We use the union bound on the BER performance of CPSC-MBM to obtain the diversity order. The minimum value of the exponent of SNR in the denominator of the pairwise error probability (PEP) expression gives the

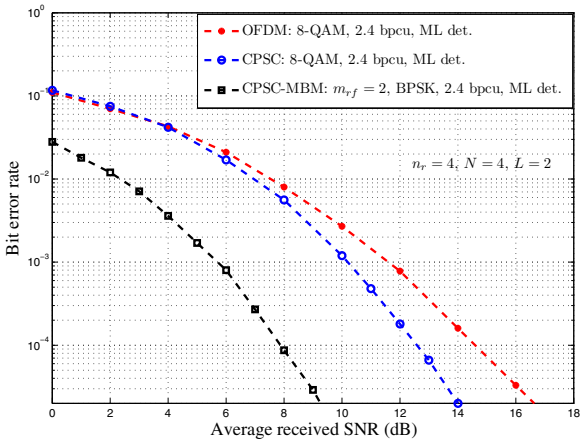

Fig. 2. BER performance of CPSC-MBM, OFDM, and CPSC schemes under ML detection at 2.4 bpcu, $N = 4$, $L = 2$, $n_r = 4$. i) CPSC-MBM: $m_{rf} = 2$, BPSK; ii) OFDM: 8-QAM; iii) CPSC: 8-QAM.

diversity order of a transmission scheme. The PEP of detecting a CPSC-MBM frame $\mathbf{x}$ as another CPSC-MBM frame $\mathbf{x}'$, given the channel matrix $\mathbf{H}$, is given by

$$P(\mathbf{x}\to\mathbf{x}'|\mathbf{H}) \quad = \quad Q(\sqrt{\mu||\mathbf{H}(\mathbf{x}-\mathbf{x}')||^2}), \tag{5}$$

where μ is a scalar multiple of the average SNR. The block circulant matrix $\mathbf{H}$ in Sec. II-C can be expressed in the form

$$\mathbf{H} \quad = \quad (\mathbf{F}^H \otimes \mathbf{I}_{n_r})\mathbf{D}(\mathbf{F}\otimes\mathbf{I}_{N_m}), \tag{6}$$

where $\otimes$ denotes the Kronecker product and $\mathbf{F}$ is the DFT matrix, given by

$$\mathbf{F} = \frac{1}{\sqrt{N}}\begin{bmatrix} \rho_{0,0}, & \rho_{0,1} & \cdots & \rho_{0,N-1} \\ \rho_{1,0} & \rho_{1,1} & \cdots & \rho_{1,N-1} \\ \vdots & \vdots & \vdots & \vdots \\ \rho_{N-1,0} & \rho_{N-1,1} & \cdots & \rho_{N-1,N-1} \end{bmatrix},$$

where $\rho_{u,v} = \exp(-j\frac{2\pi uv}{N})$, $\mathbf{D}$ is a block diagonal matrix given by

$$\mathbf{D} = \begin{bmatrix} \mathbf{D}_0 & \cdots & 0 \\ \vdots & \ddots & \vdots \\ 0 & \cdots & \mathbf{D}_{N-1} \end{bmatrix},$$

and $\mathbf{D}_q$ is given by

$$\mathbf{D}_q \quad = \quad \sum_{l=1}^{L-1}\rho_{q,l}\mathbf{H}_l = \sqrt{N}\mathbf{F}^{q,l}\otimes\mathbf{I}_{n_r}\bar{\mathbf{H}}, \tag{7}$$

where $\mathbf{F}^{q,l}$ denotes the first L elements in the qth row of $\mathbf{F}$ and $\bar{\mathbf{H}} = [\mathbf{H}_0\ \mathbf{H}_1\ \cdots\ \mathbf{H}_{L-1}]^T$. From (6), we can write

$$\begin{aligned} \mathbf{H}(\mathbf{x}-\mathbf{x}') &= (\mathbf{F}^H\otimes\mathbf{I}_{n_r})\mathbf{D}(\mathbf{F}\otimes\mathbf{I}_{N_m})(\mathbf{x}-\mathbf{x}') \\ &= (\mathbf{F}^H\otimes\mathbf{I}_{n_r})\underbrace{\begin{bmatrix} \mathbf{D}_0\mathbf{w}_0 \\ \vdots \\ \mathbf{D}_{N-1}\mathbf{w}_{N-1} \end{bmatrix}}_{\triangleq\ \mathbf{D}\mathbf{w}}, \end{aligned} \tag{8}$$

where $\mathbf{w} = [\mathbf{w}_0{}^T\ \ \mathbf{w}_1{}^T\ \ \cdots\ \ \mathbf{w}_{N-1}{}^T]$ such that $\mathbf{w}_q = \mathbf{F}^q\otimes\mathbf{I}_{N_m}(\mathbf{x}-\mathbf{x}')$ and $\mathbf{F}^q$ denotes the qth row of $\mathbf{F}$. Now, $\mathbf{D}\mathbf{w}$ can

be written as

$$\mathbf{Dw} \quad = \quad \mathbf{Vh}, \tag{9}$$

where

$$\mathbf{V} \quad = \quad \sqrt{N} \begin{bmatrix} (\mathbf{w_0}^T \otimes (\mathbf{F}^{0,L} \otimes \mathbf{I}_{n_r})) \\ \vdots \\ (\mathbf{w}_{N-1}^T \otimes (\mathbf{F}^{N-1,L} \otimes \mathbf{I}_{n_r})) \end{bmatrix}, \tag{10}$$

and $\mathbf{h}$ is the vector of all channel gains of size $Ln_rN_m \times 1$ obtained by the vectorization of $\tilde{\mathbf{H}}$. From the above equations, we obtain

$$\begin{aligned} ||\mathbf{H}(\mathbf{x}-\mathbf{x}')||^2 &= ||(\mathbf{F}^H \otimes \mathbf{I}_{n_r})\mathbf{Vh}||^2 \\ &= \mathbf{h}^H \underbrace{\mathbf{V}^H(\mathbf{F}^H \otimes \mathbf{I}_{n_r})^H(\mathbf{F}^H \otimes \mathbf{I}_{n_r})}_{\triangleq \mathbf{C}} \mathbf{Vh}, \end{aligned}$$

where $\mathbf{C}$ is a Hermitian matrix of size $Ln_rN_m \times Ln_rN_m$ whose eigen value decomposition gives

$$\mathbf{C} \quad = \quad \mathbf{U}^H \Lambda \mathbf{U}, \tag{11}$$

where $\mathbf{U}$ is a unitary matrix and Λ is a diagonal matrix having the eigen values as the diagonal elements. From (11), we can write

$$||\mathbf{H}(\mathbf{x}-\mathbf{x}')||^2 \quad = \quad \tilde{\mathbf{h}}^H \Lambda \tilde{\mathbf{h}} = \sum_{i=1}^{Ln_rN_m} \lambda_i ||\tilde{\mathbf{h}}_i||^2, \tag{12}$$

where $\tilde{\mathbf{h}} = \mathbf{Uh}$ and λ_is are the eigen values. From (5) and (12), the PEP can be written as

$$P(\mathbf{x} \to \mathbf{x}'|\mathbf{H}) = Q\left(\sqrt{\mu \sum_{i=1}^{Ln_rN_m} \lambda_i ||\tilde{\mathbf{h}}_i||^2}\right), \tag{13}$$

Applying Chernoff bound to (13), we obtain

$$P(\mathbf{x} \to \mathbf{x}'|\mathbf{H}) \leq \frac{1}{2}\exp\left(-\frac{1}{2}\mu \sum_{i=1}^{Ln_rN_m} \lambda_i ||\tilde{\mathbf{h}}_i||^2\right). \tag{14}$$

Let ρ be the number of non-zero eigen values of $\mathbf{C}$, which depends on the $\{\mathbf{x}, \mathbf{x}'\}$ pair. Let σ_i^2 be the variance of $\tilde{\mathbf{h}}_i$. The unconditional PEP can then be written as

$$\mathbb{E}_{\tilde{\mathbf{h}}}\left[\exp(-\frac{1}{2}\mu \sum_{i=1}^{Ln_rN_m} \lambda_i ||\tilde{\mathbf{h}}_i||^2)\right] = \prod_{i=1}^{\rho} \frac{1}{1+\frac{\sigma_i^2 \mu \lambda_i}{2}}. \tag{15}$$

At high SNRs, we can write the unconditional PEP as

$$P(\mathbf{x} \to \mathbf{x}') \leq \frac{2^{\rho-1}}{\mu^\rho} \prod_{i=1}^{\rho} \frac{1}{\sigma_i^2 \lambda_i}. \tag{16}$$

The PEP term corresponding to the minimum ρ will dominate the other terms in the unconditional PEP upper bound expression. Hence the minimum value of ρ among all the $\{\mathbf{x}, \mathbf{x}'\}$ pairs will give the diversity of the system.

We computed the minimum value of ρ and hence the diversity of CPSC-MBM for different values of m_{rf}, n_r, L. The results are shown in Table I. It is observed that the number of non-zero eigen values and hence the diversity order achieved in CPSC-MBM under ML detection is n_r. We have verified this predicted diversity order through simulations in Fig. 3. Figure 3 shows the BER performance of CPSC-MBM with $m_{rf} = 2$, $N = 3$, $L = 2$, BPSK, and $n_r = 1, 2$ under ML detection. We have also plotted $c1/SNR$ and $c2/SNR^2$ lines on the same graph. It is observed that, for $n_r = 1$, the simulated BER runs parallel to the $c1/SNR$ line at high SNRs, and for $n_r = 2$, the simulated BER runs parallel to the $c1/SNR^2$ line. This shows that the diversity order achieved is 1 and 2 for $n_r = 1$ and $n_r = 2$, respectively. This validates the diversity order of n_r obtained analytically.

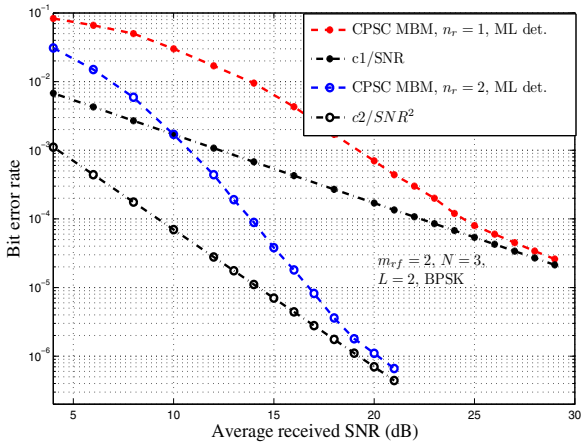

Fig. 3. Diversity order of CPSC-MBM under ML detection. $m_{rf} = 2$, $N = 3$, $L = 2$, BPSK, $n_r = 1, 2$.

IV. Message Passing Based Signal Detection

At the receiver, the detection algorithm observes $\mathbf{y}$ and estimates $\mathbf{x}$. As pointed out earlier, the ML detection of a CPSC-MBM frame has a complexity that increases exponentially in m_{rf} and N. So low complexity detection algorithms are needed for CPSC-MBM with large m_{rf} and N. In this section, we develop a message passing based low complexity algorithm suited for detection of large dimensional CPSC-MBM signals.

The proposed algorithm works on the system model given in (3). It estimates $\mathbf{x}$ given $\mathbf{y}$ and $\mathbf{H}$. Now, we have $\mathbf{x} = \begin{bmatrix}\mathbf{x}_1^T & \mathbf{x}_2^T & \cdots & \mathbf{x}_j^T & \cdots & \mathbf{x}_N^T\end{bmatrix}^T$, where $\mathbf{x}_j \in \mathbb{S}$ is the N_m-length vector transmitted in the $j+L-1$th channel use. The graphical model for the message passing algorithm consists of N variable nodes each corresponding to a $\mathbf{x}_j$, and Nn_r observation nodes each corresponding to a y_i. This graphical model is illustrated in Fig. 4. The messages passed between the variable nodes and the observation nodes are constructed as follows. The received signal y_i from (3) can be written as

$$y_i = \mathbf{h}_{i,[j]}\mathbf{x}_j + \underbrace{\sum_{l=1, l\neq j}^{N} \mathbf{h}_{i,[l]}\mathbf{x}_l + n_i}_{\triangleq\, q_{i,j}}, \tag{17}$$

where $\mathbf{h}_{i,[l]}$ is a row vector of length N_m given by $\begin{bmatrix}H_{i,(l-1)N_m+1} & H_{i,(l-1)N_m+2} & \cdots & H_{i,lN_m}\end{bmatrix}$, where $H_{i,j}$ is the entry in the ith row and jth column of $\mathbf{H}$. We approximate $q_{i,j}$ to be Gaussian with mean $\hat{\mu}_{i,j}$ and variance $\hat{\sigma}_{i,j}^2$, where

(m_{rf}, n_r)	$N=3, L=2$		$N=3, L=3$	
	eigen values	Diversity (# non-zero eigen values)	eigen values	Diversity (# non-zero eigen values)
(2,1)	12, 7 zeros	1	18, 11 zeros	1
(2,2)	12, 12, 14 zeros	2	18, 18, 22 zeros	2
(2,3)	12, 12, 12, 21 zeros	3	18, 18, 18, 33 zeros	3
(3,1)	12, 15 zeros	1	18, 23 zeros	1
(3,2)	12, 12, 30 zeros	2	18, 18, 46 zeros	2

TABLE I
DIVERSITY ORDER FOR DIFFERENT CONFIGURATIONS OF m_{rf}, n_r, L ALONG WITH THE EIGEN VALUES CORRESPONDING TO THE $\{\mathbf{x}, \mathbf{x}'\}$ PAIR GIVING THE MINIMUM ρ FOR CPSC-MBM.

$$\hat{\mu}_{i,j} = \mathbb{E}\left[\sum_{l=1, l\neq j}^{N} \mathbf{h}_{i,[l]}\mathbf{x}_l + n_i\right] = \sum_{l=1, l\neq j}^{N}\sum_{\mathbf{s}\in\mathbb{S}} \hat{p}_{li}(\mathbf{s})\mathbf{h}_{i,[l]}\mathbf{s}, \quad (18)$$

$$\hat{\sigma}^2_{i,j} = \mathrm{Var}\left(\sum_{\substack{l=1,\\ l\neq j}}^{N} \mathbf{h}_{i,[l]}\mathbf{x}_l + n_i\right)$$

$$= \sum_{\substack{l=1,\\ l\neq j}}^{N}\left(\sum_{\mathbf{s}\in\mathbb{S}} \hat{p}_{li}(\mathbf{s})\mathbf{h}_{i,[l]}\mathbf{s}\mathbf{s}^H\mathbf{h}^H_{i,[l]} - \left|\sum_{\mathbf{s}\in\mathbb{S}} \hat{p}_{li}(\mathbf{s})\mathbf{h}_{i,[l]}\mathbf{s}\right|^2\right) + \sigma^2, \quad (19)$$

where $\hat{p}_{ji}(\mathbf{s})$ denotes the a posteriori probability message computed at the variable nodes as

$$\hat{p}_{ji}(\mathbf{s}) \propto \prod_{m=1,\ m\neq i}^{Nn_r} \exp\left(\frac{-\left|y_m - \hat{\mu}_{m,j} - \mathbf{h}_{m,[j]}\mathbf{s}\right|^2}{\hat{\sigma}^2_{m,j}}\right). \quad (20)$$

The message passing schedule is as follows.

1) Initialize $\hat{p}_{ji}(\mathbf{s}) = \frac{1}{|\mathbb{S}|}$, $\forall j, i, \mathbf{s}$.
2) Compute $\hat{\mu}_{ij}$ and $\hat{\sigma}^2_{i,j}$, $\forall i, j$.
3) Compute $\hat{p}_{ji}$, $\forall j, i$.

Damping of the messages [20] is done in (20) with a damping factor $\Delta \in (0, 1]$ to improve convergence. Steps 2 and 3 are repeated for a fixed number of iterations. At the end of these iterations, the vector probabilities are computed as

$$\hat{p}_j(\mathbf{s}) \propto \prod_{i=1}^{Nn_r} \exp\left(\frac{-\left|y_i - \hat{\mu}_{i,j} - \mathbf{h}_{i,[j]}\mathbf{s}\right|^2}{\hat{\sigma}^2_{i,j}}\right), \ j = 1, 2, \ldots, N. \quad (21)$$

The estimates $\hat{\mathbf{x}}_j$s are obtained by choosing the signal vector $\mathbf{s} \in \mathbb{S}$ that has the largest APPs. That is,

$$\hat{\mathbf{x}}_j = \underset{\mathbf{s}\in\mathbb{S}}{\mathrm{argmax}}\ \hat{p}_j(\mathbf{s}). \quad (22)$$

The $\hat{\mathbf{x}}_j$s obtained are demapped to get the MAP on each channel use, which are then demapped to obtain the mirror index bits. The non-zero entry of $\hat{\mathbf{x}}_j$ is demapped to get the modulation symbol bits.

Complexity: The total complexity of the above message passing based detection algorithm is $O(n_r N|\mathbb{S}|)$, which is significantly lower compared to ML detection complexity.

Performance results: In Figs. 5 and 6, we present the BER performance of CPSC-MBM using the proposed message passing detection algorithm. The CPSC-MBM system considered in Fig. 5 has $m_{rf} = 2$, $N = 8$, $L = 2$, $n_r = 4$, BPSK, and 2.67 bpcu. A damping factor of $\Delta = 0.3$ is used in the message passing. The performance of this CPSC-MBM system is compared with those of OFDM with ML detection and CPSC for the same bpcu. Since ML detection is too complex for CPSC, a message passing algorithm similar to the one presented here is used for CPSC signal detection. The parameters taken for OFDM and CPSC are: $N = 8$, $L = 2$, $n_r = 4$, and 2.67 bpcu. From Fig. 5, we observe that, at a BER of 10^{-4}, CPSC-MBM outperforms OFDM by about 6.2 dB, and CPSC by about 4.2 dB. We see a similar performance advantage in favor of CPSC-MBM compared to OFDM and CPSC in Fig. 6, where $N = 16$ and the achieved rate is 2.82 bpcu. This shows that the proposed detection scheme scales well for large dimensions and achieves good performance. The study illustrates that MBM is a promising modulation scheme which can achieve higher rates and better performance through RF mirror indexing.

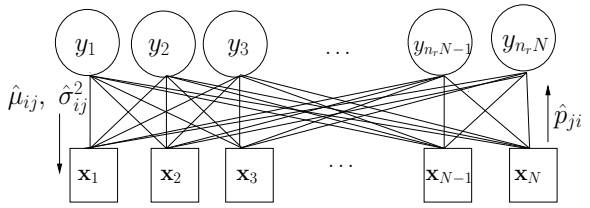

Fig. 4. The graphical model and messages in the proposed messaging passing algorithm for CPSC-MBM signal detection.

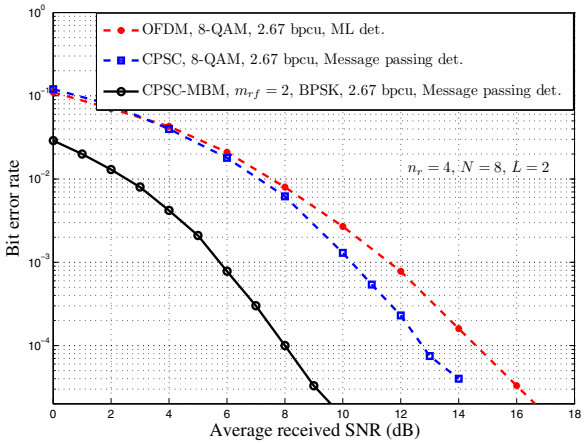

Fig. 5. BER performance comparison of CPSC-MBM using the proposed message passing detection with that of OFDM with ML detection and CPSC with message passing detection at 2.67 bpcu, $N = 8$, $L = 2$, $n_r = 4$. *i*) CPSC-MBM: $m_{rf} = 2$, BPSK; *ii*) OFDM: 8-QAM; *iii*) CPSC: 8-QAM.

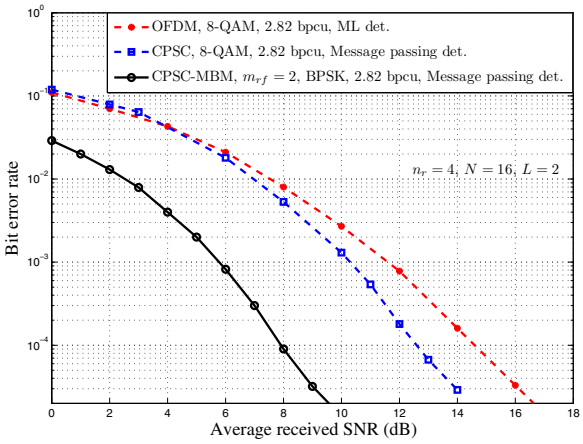

Fig. 6. BER performance comparison of CPSC-MBM using the proposed message passing detection with that of OFDM with ML detection and CPSC with message passing detection at 2.82 bpcu, $N = 16$, $L = 2$, $n_r = 4$. i) CPSC-MBM: $m_{rf} = 2$, BPSK; ii) OFDM: 8-QAM; iii) CPSC: 8-QAM.

V. Conclusion

We investigated media-based modulation (MBM), a recent and promising modulation scheme that uses RF mirrors to 'modulate the channel' to convey information bits through indexing of these mirrors. We considered a cyclic-prefix single-carrier MBM (CPSC-MBM) scheme in ISI channels, which has not been reported before. Our study showed that, for the same spectral efficiency, CPSC-MBM performed better than conventional OFDM and CPSC schemes. We presented a diversity analysis of CPSC-MBM and validated the analytically obtained diversity orders through simulations. We also presented a message passing based algorithm for the detection of CPSC-MBM signals. The proposed algorithm scaled well in complexity and achieved good performance. Channel estimation, effect of imperfect knowledge of the channel alphabet at the receiver, effect of spatial correlation, and multi-antenna systems with CPSC-MBM are interesting topics for further investigation.

References

[1] B. Schaer, K. Rambabu, J. Borneman, and R. Vahldieck, "Design of reactive parasitic elements in electronic beam steering arrays," *IEEE Trans. Ant. and Propagat.*, vol. 53, no. 6, pp. 1998-2003, Jun. 2005.

[2] C. Sun and N. C. Karmakar, "Direction of arrival estimation with a novel single-port smart antenna," *EURASIP J. Applied Signal Process.*, 2004, 2004:9, 1364-1375.

[3] R. Vaughan, "Switched parasitic elements for antenna diversity," *IEEE Trans. Ant. and Propagat.*, vol. 47, no. 2, pp. 399-405, Feb. 1999.

[4] J. Costantine, Y. Tawk, S. E. Barbin, and C. G. Christodoulou, "Reconfigurable antennas: design and applications," *Proceedings of the IEEE*, vol. 103, no. 3, pp. 424-437, Mar. 2015.

[5] O. N. Alrabadi, A. Kalis, C. B. Papadias, R. Prasad,"Aerial modulation for high order PSK transmission schemes," in *Wireless VITAE 2009*, May 2009, pp. 823-826.

[6] R. Bains, "On the usage of parasitic antenna elements in wireless communication systems," Ph.D. Thesis, Department of Electronics and Telecommunications, Norwegian University of Science and Technology, May 2008. Online: http://ntnu.diva-portal.org/smash/get/diva2:124527/FULLTEXT01.pdf

[7] A. K. Khandani, "Media-based modulation: A new approach to wireless transmission," in *Proc. IEEE ISIT'2013*, Jul. 2013, pp. 3050-3054.

[8] A. K. Khandani, "Media-based modulation: Converting static Rayleigh fading to AWGN," in *Proc. IEEE ISIT'2014*, Jun-Jul. 2014, pp. 1549-1553.

[9] A. K. Khandani, "Media-based modulation: A new approach to wireless transmission," Tech. Rep., University of Waterloo, Canada. Online: http://www.cst.uwaterloo.ca/reports/media-report.pdf

[10] E. Seifi, M. Atamanesh, and A. K. Khandani, "Media-based modulation: A new frontier in wireless communications," online: arXiv:1507.07516v3 [cs.IT] 7 Oct. 2015.

[11] Y. Naresh and A. Chockalingam, "On media-based modulation using RF mirrors," *Proc. ITA'2016*, San Diego, Feb. 2016. Accepted in *IEEE Trans. Veh. Tech.* Available in IEEE Xplore DOI: 10.1109/TVT.2016.2620989.

[12] M. Di Renzo, H. Haas, A. Ghrayeb, S. Sugiura, and L. Hanzo, "Spatial modulation for generalized MIMO: challenges, opportunities and implementation," *Proc. of the IEEE*, vol. 102, no. 1, pp. 56-103, Jan. 2014.

[13] J. Wang, S. Jia, and J. Song, "Generalized spatial modulation system with multiple active transmit antennas and low complexity detection scheme," *IEEE Trans. Wireless Commun.*, vol. 11, no. 4, pp. 1605-1615, Apr. 2012.

[14] H. Sari, G. Karam, and I. Jeanclaude, "Transmission techniques for digital terrestrial TV broadcasting," *IEEE Commun. Mag.*, vol. 33, no. 2, pp. 100-109, Feb. 1995.

[15] D. Falconer, S. L. Ariyavisitakul, A. Benyamin-Seeyar, and B. Eidson, "Frequency domain equalization for single-carrier broadband wireless systems," *IEEE Commun. Mag.*, vol. 40, no. 4, pp. 58-66, Apr. 2002.

[16] N. Benvenuto and S. Tomasin, "On the comparison between OFDM and single carrier modulation with DFE using a frequency-domain feedforward filter," *IEEE Trans. Commun.*, vol. 50, no. 6, pp. 947-955, Jun. 2002.

[17] Z. Wang, X. Ma, and G. B. Giannakis, "OFDM or single-carrier block transmissions?," *IEEE Trans. Commun.*, vol. 52, no. 3, pp. 380-394, Mar. 2004.

[18] B. Devillers and L. Vandendorpe, "Bit rate comparison of adaptive OFDM and cyclic prefixed single-carrier with DFE," *IEEE Commun. Lett.*, vol. 13, no. 11, pp. 838-840, Nov. 2009.

[19] D. Tse and P. Viswanath, *Fundamentals of Wireless Communications*, Cambridge Univ. Press, 2005.

[20] M. Pretti, "A message passing algorithm with damping," *J. Statist. Mech.: Theory Practice*, p. 11008, Nov. 2005.